X International Conference on Structural Dynamics, EURODYN 2017

Investigation of the effect of directivity pulses on the seismic response of a curved RC bridge

Vasileios Angelidakis, Vassiliki Kardoutsou*, Ioannis Psycharis, Ioannis Taflampas

School of Civil Engineering, National Technical University of Athens, Heroon Polytechneiou 9, Zografou 15780, Greece

Abstract

Within the near-fault zone, ground motions are influenced by the rupture mechanism and directivity phenomena. Near-fault ground motions are of special interest in Earthquake Engineering, as they might result in large inelastic displacements of structures. In this paper, an investigation is presented concerning the effect of the directivity pulses inherent in near-fault ground motions on the inelastic response of a curved RC bridge, specifically Bridge G7 of Egnatia Highway in Greece. The analyses were performed for a sample of 90 near-fault seismic records. From each record, the first six pulses were extracted and simplified 'pulse records' were defined, composed of one or more (up to six) pulses. First, a pushover analysis was performed and, based on the derived yield acceleration corresponding to the bilinear representation of the capacity curve, each record was scaled to three intensity levels, corresponding to behavior factors q_y = 2, 3 and 4. Non-linear time-history analyses were then performed for each original record and the related 'pulse records' using OpenSees. By comparing the results, conclusions were drawn on the significance of each pulse to the nonlinear response. To this end, the errors for several general and local response quantities were calculated. The results show that the maximum inelastic deformations occur for the ground motions for which the elastic fundamental period of the bridge is close to one half of the period of the predominant pulse. Also, in most cases, the maximum response for the original record could be adequately estimated by the response for the 'pulse record' consisted of only two (and in few cases of three) pulses, especially when the fundamental period of the bridge was in between the periods of these pulses.

1. Introduction

A characteristic feature of near-fault ground motions concerns discrete directivity pulses inherent in the ground motion time-histories, which are obvious in the ground velocity time-history. Ground motions affected by forward directivity effects have been the subject of systematic studies in the last decades. Several researchers have isolated

* Corresponding author. Tel.: +30-210-772-1171.
  E-mail address: vkardcv@gmail.com

the most significant characteristics of the seismic action near active faults and their effect on the elastic and inelastic response, mainly for *SDOF* systems. In what concerns the elastic response, Shahi and Baker [1] observed a bell-shaped amplification of the elastic spectral values around the period of the predominant pulse, T_p. For inelastic response, Tothong and Cornell [2] observed increased values of the ratio of the ductility over the behavior factor, μ/q, for structures with period around one half of the period of the predominant pulse.

In this paper, an extension of this investigation to include not only the predominant pulse, but also other significant pulses (up to six) inherent in near-fault ground motions, is presented. Analyses were performed for a curved bridge and for a sample of 90 near-fault seismic records classified as pulse-like in the literature.

It is reminded that, as common practice (Mavroeidis and Papageorgiou [3], Baker [4]), the identification and the extraction of the significant directivity pulses is performed through wavelet analyses, using idealized wavelet forms for their mathematical representation. In the present investigation, the Mavroeidis and Papageorgiou [3] wavelet was used for the representation of the six most significant pulses in each record, which were identified by applying the Mimoglou *et al.* [5] methodology.

It should be noted that recent studies have proposed the approximation of near-fault ground motions by synthesized records constructed from the superposition of idealized pulses (Lu and Panagiotou [6]). To this end, this study was focused on the number of significant pulses required to adequately estimate the inelastic response of the considered bridge, compared with the non-linear time history (NLTH) response for the original record.

2. Structure considered

All the analyses were performed for the case study of an existing curved three-span bridge, specifically Bridge G7 of Egnatia Highway, Greece. The overall length of the bridge is 270.00 m, consisting of two end spans of 75.00 m each and a central span of 120.00 m. In plan, the bridge lies on a circular arc of radius 320 m. Vertically, the red line of the highway forms an arc of radius 1000 m, which creates a height difference of 6.5 m between the end sections of the deck. A general view of the bridge is presented in Fig. 1.

The deck is connected monolithically to the mid-piers and has a heavily post-tensioned single-cell box cross section of variable height. The mid-piers M1 and M2 are of height 41.70 m and 49.50 m, respectively, and share a hollow rectangular cross section with outer dimensions of 4.00 m × 7.35 m and thickness 0.75 m. Typical cross sections of the deck and the piers are presented in Fig. 1. Both the deck and the piers are made of concrete of grade C35/45. The reinforcement is of grade S500s and the number of the longitudinal rebars of the piers is consistent throughout their height and equal to 252 Ø28 ($\rho \approx 1.05\%$).

The deck is supported by the abutments through elastic single-point pot bearings, which allow its free sliding in the longitudinal direction, while in the transverse direction the motion of the deck is restrained by shear keys, which, however, break for seismic loads larger than the design ones.

The piers are founded on circular concrete shafts of diameter 10.00 m and height 15.00 m.
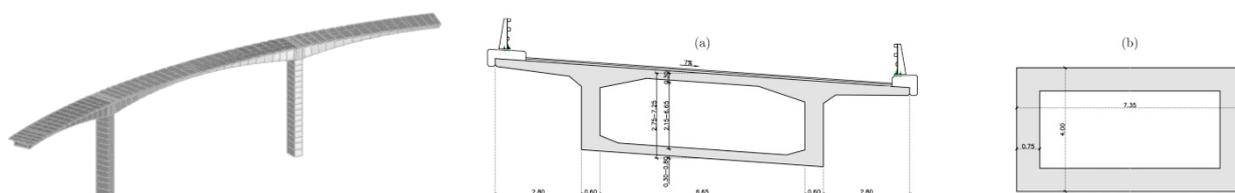

Fig. 1: General view of the bridge considered in the analyses & typical cross sections of the deck (a) and the piers (b).

3. Numerical model

The structure was simulated in the open-source software OpenSees [6]. The deck of the bridge was modelled using Elastic Beam-Column Elements, since formation of plastic hinges is expected only at the piers.

The piers M1 and M2 were supposed fixed at their base, considering the foundation type and the rocky soil conditions. For their modelling, force-based beam-column elements were used. The fibers of the sections were

assigned with uniaxial material constitutive laws, which defined their monotonic and cyclic behavior. Mean values were considered for the properties of the materials, as typical in non-linear analyses. In Fig. 2, the discretization of a typical fiber section of the piers is presented, along with the stress-strain curves of the materials considered.

The behavior of the reinforcing steel was simulated using the Steel02 material of OpenSees. The cover-concrete inside and outside the confined cores of each section was simulated using the Concrete01 material of OpenSees. Zero residual strength was considered, in order to simulate the spalling of the cover concrete. The confined concrete was simulated using the Concrete04 material of OpenSees and its characteristics were computed using the stress-strain model proposed by Mander *et al.* [8]. Due to different spacing of the transverse reinforcement along the height of the piers, and, consequently, the different provided lateral confining stress, three different cases of confined concrete were defined, as shown in Fig. 2 (a).
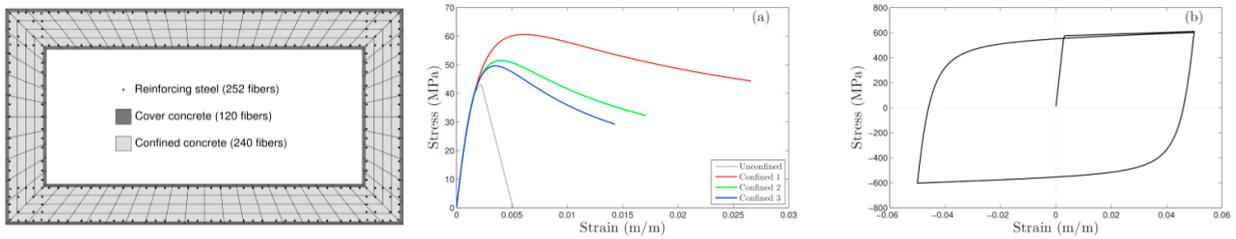

Fig. 2: Typical fiber section of the piers & constitutive laws used to model the behavior of the materials: (a) Monotonic behavior for the cover and the confined cores' concrete material; (b) Cyclic behavior of the reinforcing steel material.

The abutments A1 and A2 were considered rigid in their long direction (transverse direction of the bridge), due to their corresponding large stiffness. Thus, and taking under consideration the free sliding in the longitudinal direction of the bridge, the abutments were not included in the model of the structure; instead, appropriate boundary conditions were applied at the ends of the bridge: free sliding in the longitudinal direction and restriction of motion in the transverse direction, due to the presence of the shear keys; the latter were modeled as Zero-Length Elements with very large elastic stiffness. It must be noted that due to the plan curvature of the deck and the existence of shear keys at the abutments, the transverse and longitudinal displacements are partially interacting, resulting to biaxial bending conditions at the piers, for every horizontal movement of the deck.

4. Static Pushover Analysis

Firstly, the main features of the inelastic behavior of the structure were assessed from the capacity curve computed through a Static Pushover (SPO) Analysis. Throughout this paper, only the response of the bridge in the longitudinal direction is considered, thus, the SPO analysis was performed for horizontal loads that followed the dominant eigenmode in this direction. From the corresponding capacity spectrum the idealized bilinear (elastic-perfectly plastic) behavior was derived (Fig. 3) following the FEMA 273 [9] procedure and the yield parameters of the equivalent SDOF system were determined: yield acceleration $S_{ay} = 1.811$ m/s^2, yield displacement $S_{dy} = 0.225$ m and elastic period $T^* = 2.215$ s.
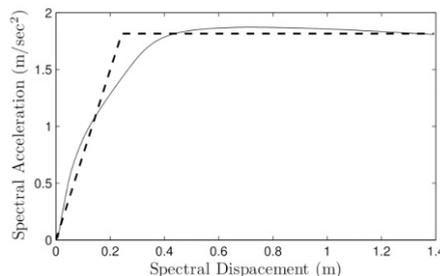

Fig. 3: Capacity Spectrum of the equivalent *SDOF* system (longitudinal direction).

5. Ground motions and corresponding pulses

A sample of 90 near-fault seismic records of magnitude ranging from M_w = 5.0 to 7.4 was selected for the analyses. From these, 55 are classified as pulse-like by Baker [4], while the rest 35 are classified as pulse-like according to the methodology proposed by Kardoutsou *et al.* [10]. For each ground motion, the first six significant pulses P_i (i = 1 to 6) were extracted by applying the methodology described in Mimoglou *et al.* [5] and using the Mavroeidis and Papageorgiou [3] wavelet for the mathematical representation of the pulses. Then, the 'pulse records' S_1 to S_6 were constructed from the first pulse only (S_1), or by superimposing the first two (S_2), the first three (S_3), and so on up to all six (S_6) pulses. An example is shown in Fig. 4.
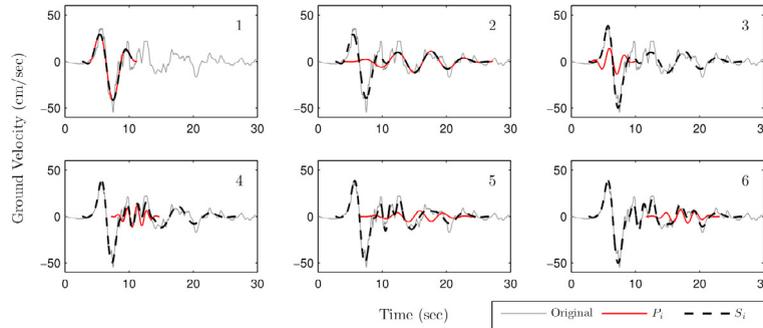

Fig. 4: Velocity time histories of the first six significant pulses, P_i, and the corresponding pulse records, S_i, for the EC County FF station record of the Imperial Valley, 1979 Earthquake. The original record is shown with grey line.

6. Non-Linear Time History Analyses

6.1. Scaling of the records

Analyses were performed for three intensity levels of each record that correspond to behavior factor q_y = 2, 3 and 4. Specifically, for each q_y value, each ground motion and its corresponding 'pulse records' were multiplied by the following scaling factor, *SF*:

$$SF = q_y \cdot \frac{S_{ay}}{S_{a,el}(T^*)} \tag{1}$$

where S_{ay} and T^* are the yield acceleration and the period of the equivalent *SDOF* system, respectively, (defined in Section 4) and $S_{a,el}(T^*)$ is the elastic pseudo-acceleration for period $T = T^*$ and 5% damping that corresponds to the original record.

6.2. Maximum response quantities

In order to investigate the effect of directivity phenomena on the non-linear response and examine whether the original ground motions could be substituted by the simpler 'pulse records', at least in what concerns the estimation of the expected damage, the following response quantities, which are associated with damage, were examined:

- The maximum ductility, μ, that develops during the seismic motion, measured in terms of the equivalent *SDOF* system, specified as the ratio of the maximum displacement, S_{du}, over the corresponding yield displacement, S_{dy}. The yield displacement S_{dy} was defined in Section 4, while the maximum displacement S_{du} of the equivalent *SDOF* system was determined from the maximum displacement of the reference point of the bridge, as calculated from the NLTH analyses.
- The maximum drift ratios of the piers that develop during the seismic motion.
- The maximum curvatures that develop during the seismic motion at the edge sections of the piers.

6.3. Results

The results obtained for the original records are presented in Fig. 5, in which the variation of the aforementioned quantities versus the period ratio T^*/T_{p1} is presented, with T_{p1} being the period of the predominant pulse of each record, which corresponds to the peak of the convolution spectrum $S_v \times S_d$ for 5% damping, as introduced by Mimoglou *et al.* [5]. The solid lines correspond to the moving average of the scattered data for each behavior factor q_y, produced through locally weighted regression analysis.

It is observed that the maximum inelastic response occurs when the period of the predominant pulse is double the period of the structure ($T^*/T_{p1} \approx 0.5$) and the minimum when $T_{p1} \approx T^*$. As shown in Fig. 5(a), for $T^*/T_{p1} \approx 0.5$ the required ductility μ is significantly larger than the corresponding behavior factor q_y, thus, the equal displacement rule does not hold. A similar conclusion was found by Tothong and Cornell [2] for *SDOF* structures.

As a second step, it was investigated whether simplified 'pulse records' could be used instead of the original records to produce similar maximum values of the examined response quantities. More specifically, the investigation aimed at finding the number of significant pulses that, if superposed into a 'pulse record', can adequately approximate the maximum response of the structure. The efficiency of each 'pulse record' S_i ($i = 1$ to 6) was measured from the produced error $er_i(R_j)$ to the response quantity R_j, calculated by:

$$er_i = \frac{R_j(S_i) - R_j(orig)}{R_j(orig)} \tag{2}$$

where $R_j(orig)$ is the response quantity R_j calculated for the original record and $R_j(S_i)$ the corresponding value calculated for the 'pulse record' S_i.

Moving averages of the errors produced by the use of 'pulse records' S_1, S_2, S_3 and S_6 in case of $q_y = 4$ versus the period ratio T^*/T_{p1} are presented in Fig. 6. The errors are shown with their absolute value, since it was observed that their sign did not follow any specific trend indicating underestimation or overestimation of the response. The respective graphs for intensity levels $q_y = 2$ and $q_y = 3$ are not presented, as they show similar behavior.
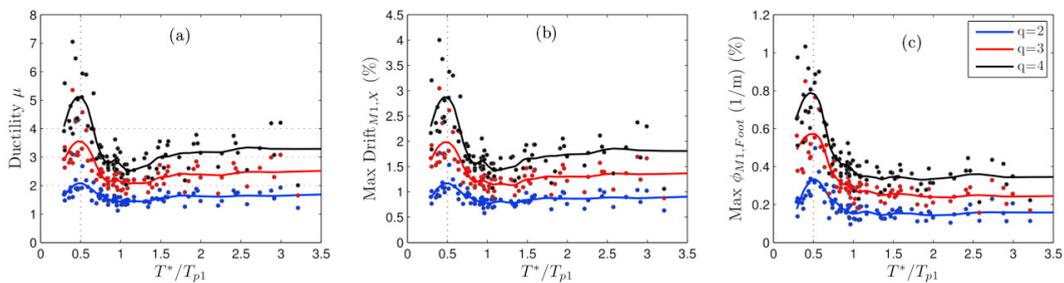

Fig. 5: Maximum response quantities of the structure for the three intensity levels: (a) Ductility of the equivalent *SDOF*; (b) Maximum drift of Pier M1; (c) Maximum Curvature at the base of pier M1. Solid lines correspond to the moving average of the obtained data.
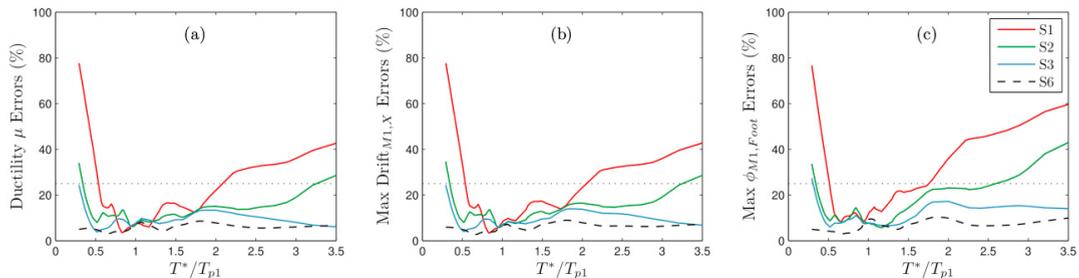

Fig. 6: Moving averages of the absolute values of the errors produced using 'pulse records' S_1, S_2, S_3 and S_6 for $q_y = 4$: (a) Ductility of the equivalent *SDOF*; (b) Maximum drift of pier M1; (c) Maximum curvature at the base of pier M1.

Adopting an acceptable error level of 25% (shown with a dotted line on the graphs of Fig. 6), it is observed that the first pulse alone (record S_1) can adequately predict the maximum inelastic response if $0.6 < T^*/T_{p1} < 2.0$. For structures with period outside this range, the produced error is significant. Thus, the first pulse alone cannot be unconditionally used as a sufficient 'pulse record', a conclusion that was also derived by Lu and Panagiotou [6].

If the second pulse is included in the 'pulse record' (S_2), the range of periods in which acceptable results are obtained increases significantly: errors less than 25% are obtained for $0.3 < T^*/T_{p1} < 3.0$. Interesting to note that the accuracy achieved for T^* close to T_{p1} does not improve.

Increasing even more the number of pulses considered (three or more) results in better accuracy only for large values of the period ratio T^*/T_{p1}, more than 3.0. Taking under consideration that, for typical near-fault records, the value of T_{p1} is usually larger than 1.5 s, this improvement concerns only very flexible structures with significantly large period T^*. Therefore, it can be concluded that, in most cases, the use of a 'pulse record' that consists of the two first pulses is adequate. Interesting to note that the minimum errors were observed when the period of the structure T^* was in between the periods of the considered two pulses, T_{p1} and T_{p2}.

7. Conclusions

In this study, the effect of the directivity pulses inherent in near-fault ground motions on the inelastic response of a curved RC bridge is investigated. Analyses were performed for a sample of 90 near-fault ground motions, for which the first six significant pulses were identified and extracted. Superposing these pulses sequentially, six synthesized 'pulse records' were constructed for each considered ground motion. NLTH analyses were performed for the original record and the constructed 'pulse records' and for three intensity levels. Thus, conclusions were drawn concerning the accuracy obtained by using the simplified 'pulse records' instead of the original ground motion.

The results show that near-fault phenomena might result in significant amplification of the inelastic response, which maximizes in case of structures with period close to one half the period of the predominant pulse.

Concerning the synthesized 'pulse records', it was found that the predominant pulse alone can predict the inelastic response with acceptable accuracy (error less than 25%) only for structures with period larger than 60% of the period of the pulse and less than twice the pulse period. Outside this range of periods, the addition of the second pulse is usually adequate, except of very flexible structures with period larger than $3T_{p1}$, for which the pulse record must include at least the three first pulses.

References

[1]   S.K. Shahi, J.W. Baker, An empirically calibrated framework for including the effects of near-fault directivity in probabilistic seismic hazard analysis, Bulletin of the Seismological Society of America, 101(2) (2011) 742–755.
[2]   P. Tothong, C.A. Cornell, Probabilistic seismic demand analysis using advanced ground motion intensity measures, attenuation relationships, and near-fault effects, PEER Report 2006/11, Pacific Earthquake Engineering Research Center, University of California, Berkeley, CA, 2006.
[3]   G.P. Mavroeidis, A.S. Papageorgiou, A mathematical representation of near-fault ground motions, Bulletin of the Seismological Society of America, 93 (2003) 1099–1131.
[4]   J.W. Baker, Quantitative classification of near-fault ground motions using wavelet analysis, Bulletin of the Seismological Society of America, 97 (2007) 1486–1501.
[5]   P. Mimoglou, I.N. Psycharis, I.M. Taflampas, Explicit determination of the pulse inherent in pulse-like ground motions, Earthquake Engineering and Structural Dynamics, 43 (2014) 2261–2281.
[6]   Y. Lu, M. Panagiotou, Characterization and representation of strong near-fault ground motions using wavelet-based cumulative pulse extraction, Tenth U.S. National Conference on Earthquake Engineering Frontiers of Earthquake Engineering, Anchorage, Alaska, July 21-25, 2014.
[7]   F. McKenna, G.L. Fenves, M.H. Scott, B. Jeremic, Open system for earthquake engineering simulation (OpenSees), Pacific Earthquake Engineering Research Center, University of California, Berkeley, CA, 2000.
[8]   J.B. Mander, M.J.N. Priestley, R. Park, Theoretical stress-strain model for confined concrete, Journal of Structural Engineering, American Society of Civil Engineers, 114(8) (1988) 1804-1826.
[9]   Federal Emergency Management Agency, NEHRP Guidelines for the seismic rehabilitation of buildings, FEMA Publication No. 273, Washington, D.C, 1997.
[10]   V. Kardoutsou, P. Mimoglou, I. Taflampas, I.N. Psycharis, Evaluation and comparison of new methods for the classification of ground motions as pulse-like or non pulse-like, SECED 2015 Conference: Earthquake Risk and Engineering towards a Resilient World, Cambridge, UK, July 9-10, 2015.